CHEMISTRY
A EUROPEAN JOURNAL

ChemPubSoc
Europe

DOI: 10.1002/chem.201301822

High CO_2-Capture Ability of a Porous Organic Polymer Bifunctionalized with Carboxy and Triazole Groups

Lin-Hua Xie and Myunghyun Paik Suh*[a]

Abstract: A new porous organic polymer, **SNU-C1**, incorporating two different CO_2-attracting groups, namely, carboxy and triazole groups, has been synthesized. By activating **SNU-C1** with two different methods, vacuum drying and supercritical-CO_2 treatment, the guest-free phases, **SNU-C1-va** and **SNU-C1-sca**, respectively, were obtained. Brunauer–Emmett–Teller (BET) surface areas of **SNU-C1-va** and **SNU-C1-sca** are 595 and 830 m^2g^{-1}, respectively, as estimated by the N_2-adsorption isotherms at 77 K. At 298 K and 1 atm, **SNU-C1-va** and **SNU-C1-sca** show high CO_2 uptakes, 2.31 $mmol\,g^{-1}$ and 3.14 $mmol\,g^{-1}$, respectively, the high level being due to the presence of abundant polar groups (carboxy and triazole) exposed on the pore surfaces. Five separation parameters for flue gas and landfill gas in vacuum-swing adsorption were calculated from single-component gas-sorption isotherms by using the ideal adsorbed solution theory (IAST). The data reveal excellent CO_2-separation abilities of **SNU-C1-va** and **SNU-C1-sca**, namely high CO_2-uptake capacity, high selectivity, and high regenerability. The gas-cycling experiments for the materials and the water-treated samples, experiments that involved treating the samples with a CO_2-N_2 gas mixture (15:85, *v/v*) followed by a pure N_2 purge, further verified the high regenerability and water stability. The results suggest that these materials have great potential applications in CO_2 separation.

Keywords: carbon dioxide capture · click reactions · porous organic polymers · vacuum-swing adsorption

Introduction

The dramatic increase in the amount of greenhouse gases (GHGs), such as CO_2, CH_4, and N_2O, in atmosphere, an increase that began during the Industrial Revolution, is generally believed to be responsible for global warming and climate change. While all other GHGs with a mass similar to that of CO_2 have a much higher greenhouse effect than CO_2 itself, the concentration of CO_2 in the atmosphere is the highest among all the GHGs and is responsible for approximately 60% of the global-warming effect.[1] The major source of anthropogenic CO_2 emissions is the combustion of fossil fuels, a process that will continue to be used in the coming decades. Therefore, carbon dioxide capture and storage (CCS) technologies need to be developed to reduce the concentration of CO_2 in the atmosphere.[2] Although some technologies are already available for CO_2 capture, such as the use of amine scrubbers and cryogenic separation, the large energy penalties associated with these technologies limit their large-scale application.[3] Alternative CO_2-capture materials are solid adsorbents such as activated-carbon materials,[4] zeolites,[5] metal–organic frameworks (MOFs),[6,7] and porous organic materials,[8–11] which physisorb CO_2 through relatively weak van der Waals forces. The weak interactions between CO_2 and the internal surface of the solid adsorbents make regeneration of the materials energy efficient. In addition, the sorption performance of the solid adsorbents can be optimized by tuning their overall structural topologies or local functionalities.

In developing solid adsorbents, current major research efforts are focused on improving CO_2-sorption capacity and selectivity of the materials at ambient temperature. One of the most extensively studied strategies is the introduction of alkylamine groups to the solid adsorbents.[12–14] The introduction of alkylamine groups to the adsorbents results in increased CO_2-sorption capacities and excellent selectivity, despite the surface areas being lower than those of the parent materials. To fully regenerate the alkylamine-functionalized adsorbents, additional heating is necessary owing to the chemical reactions between the introduced alkylamines and CO_2. Temperature-swing adsorption (TSA) has been generally adapted to optimally use them. However, for practical applications, vacuum-swing adsorption (VSA) is preferred over TSA and pressure-swing adsorption (PSA) because TSA involves slow heating and cooling steps and PSA involves pressurizing the large feed stream, a process that is cost prohibitive.[15] Therefore, there are drawbacks in introducing alkylamines and other highly CO_2-attracting functionalities to the solid adsorbents. It has been demonstrated that some polar functional moieties, such as $-NO_2$,[16] -OH,[17,18] -COOH,[19] $-SO_3H$,[20] arylamines,[21] and heterocyclic nitrogen atoms,[22–24] incorporated into the porous mate-

[a] Dr. L.-H. Xie, Prof. M. P. Suh
Department of Chemistry, Seoul National University
Seoul 151-747 (Republic of Korea)
Fax: (+82) 2-886-8516
E-mail: mpsuh@snu.ac.kr

Supporting information for this article is available on the WWW under http://dx.doi.org/10.1002/chem.201301822.

rials enhance CO_2 affinities because of the high quadrupole moment (14.3×10^{-4} C m^2) and polarizability (26.3×10^{-25} cm^3) of CO_2.[25] The adsorbents containing these moderately CO_2-attracting functionalities have their advantages in that they can be readily regenerated after CO_2 adsorption because no chemisorption is involved. Although MOF materials are some of the most intensively investigated solid adsorbents in recent years, they are often very unstable toward moisture. Therefore, porous organic polymers (POPs) have recently attracted attention.[26–33] In general, POPs show good mechanical, thermal, and chemical stability because of the covalent bonding nature of the networks, and they are regarded as highly promising materials for practical CO_2-capture applications.

With these considerations in mind, we planned to develop energy-efficient CO_2-capture materials by synthesizing POPs that contain moderately CO_2-attracting groups covering the pore surfaces as densely as possible (Scheme 1). We have prepared a POP by using the copper-catalyzed 1,3-dipolar azide–alkyne cycloaddition (CuAAC) reaction, a popular type of click reaction (Scheme 2).)[34,35] The POP contains two different types of moderately CO_2-attracting groups, that is, carboxy and triazole groups. To our knowledge, all the POPs reported so far contain either none or, at most, only one type of moderately CO_2-attracting group. Single-component gas-sorption data, calculated separation parameters, and gas-cycling experiments suggest that this POP material has great potential applications in postcombustion CO_2 capture and in landfill-gas separation. It was also shown that porosity and sorption performance of this POP are significantly affected by the activation method, either vacuum drying or supercritical-CO_2 treatment, similarly to the cases of metal–organic frameworks.[36,37]

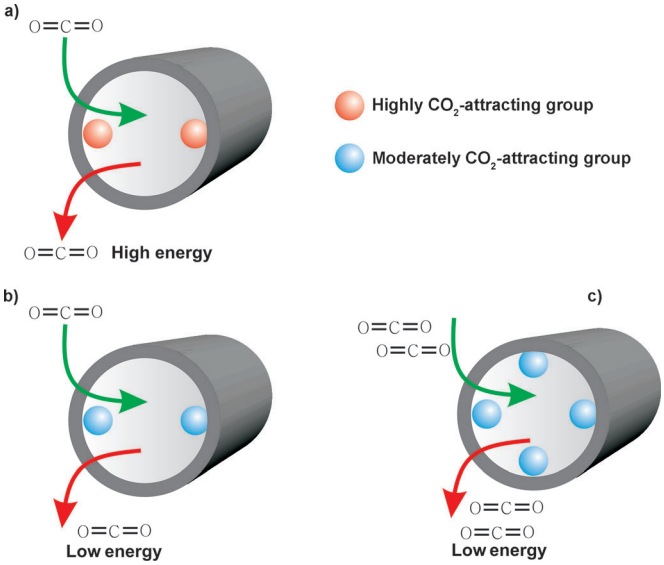

Scheme 1. Schematic representation of porous materials functionalized with a) highly CO_2-attracting groups, b) moderately CO_2-attracting groups, and c) densely distributed moderately CO_2-attracting groups.

Results and Discussion

Synthesis, activation, and general characterization: The CuAAC click reaction between 3,5-diazidobenzoic acid (**Hdab**) and 1,3,5,7-tetrakis(4-ethynylphenyl)adamantane (**tepa**) afforded a porous polymer, **SNU-C1** (caution: azides are potentially explosive). The guest solvent molecules of as-synthesized **SNU-C1** were removed by two different activation methods, room-temperature vacuum drying and supercritical-CO_2 treatment. The color of vacuum activated

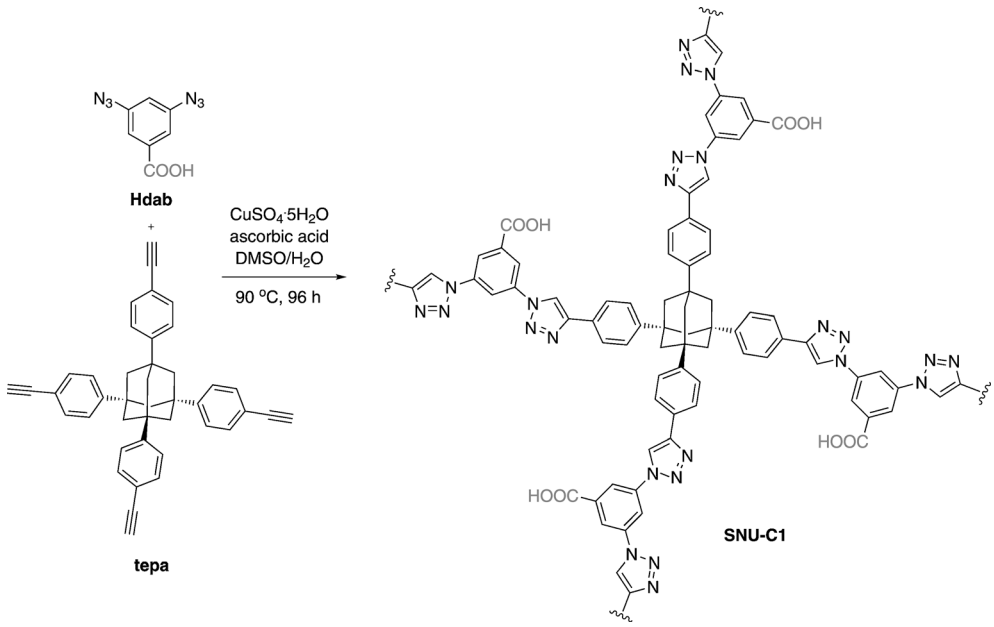

Scheme 2. Synthesis of **SNU-C1**.

SNU-C1 (**SNU-C1-va**) was orange and that of supercritical-CO_2 activated **SNU-C1** (**SNU-C1-sca**) was pale yellow (see Figure S1 in the Supporting Information). **SNU-C1-va** and **SNU-C1-sca** are insoluble in water and in all tested common organic solvents, thus suggesting that they have polymeric structures. Scanning electron microscopy (SEM) images showed that the size of the polymer particles was about 10–30 nm (see Figure S1 in the Supporting Information). The powder X-ray diffraction (PXRD) patterns revealed the amorphous nature of the samples. The infrared spectrum of the **SNU-C1** samples showed bands at around 2115 cm^{-1}, which were assigned to unreacted azide groups and have also been reported for other reported POPs prepared using CuAAC click reactions (see Figure S2 in the Supporting Information).[38–40] The presence of strong bands at 1710 cm^{-1} in the infrared spectra reveal that the carboxy groups remain intact during the reaction. Solid-state ^{13}C CP MAS NMR spectra of **SNU-C1-va** and **SNU-C1-sca** showed broad peaks around 38, 125, 137, 148, and 165 ppm (see the Supporting Information, Figure S3), which are consistent with the structures. The POP is weakly acidic in water owing to the carboxy groups. When **SNU-C1-va** (0.132 g) was immersed in degassed water (20 mL) under an N_2 atmosphere, the pH value of the suspension was 4.3. Thermogravimetric analysis revealed that **SNU-C1-va** and **SNU-C1-sca** lost water molecules adsorbed from air below 80 °C (see Figure S4 in the Supporting Information). No apparent weight change was observed in the range 80–160 °C. Continued weight loss at higher temperatures is assumed to be due to gradual decomposition of the porous polymer.

Gas sorption properties: To evaluate the porosity of **SNU-C1-va** and **SNU-C1-sca**, N_2-adsorption isotherms were measured at 77 K (Figure 1). The N_2-adsorption isotherm of **SNU-C1-va** indicated Brunauer—Emmett–Teller (BET) and Langmuir surface areas of 595 and 602 $m^2 g^{-1}$, respectively. Dubinin–Radushkevich (DR) micropore analysis suggested a micropore volume of 0.24 $cm^3 g^{-1}$ with an average micropore width of 12.9 Å. Pore-size distribution calculated by nonlocal density-functional theory (NLDFT)[41] suggested that the material contained 10–20 Å micropores (0.24 $cm^3 g^{-1}$), 23–43 Å mesopores (0.05 $cm^3 g^{-1}$), and sparse macropores (0.04 $cm^3 g^{-1}$) (see Figure S8 in the Supporting Information). **SNU-C1-sca** showed much higher porosity than **SNU-C1-va**, having BET and Langmuir surface areas of 830 and 839 $m^2 g^{-1}$, respectively, as estimated from its N_2-adsorption isotherm at 77 K. DR micropore analysis suggested a micropore volume of 0.36 $cm^3 g^{-1}$ with an average micropore width of 16.5 Å. The results of NLDFT calculation suggested that **SNU-C1-sca** contained 10–19.5 Å micropores (0.31 $cm^3 g^{-1}$), 24–34 Å mesopores (0.18 $cm^3 g^{-1}$), and widespread macropore pores (0.78 $cm^3 g^{-1}$) (see Figure S8 in the Supporting Information).

The N_2-adsorption results reveal that the activation method used significantly affects the pore features of the POP. The macropores in POPs are commonly believed to be interparticle cavities generated by aggregation of particles within the material.[26,40] The large macropore volume of **SNU-C1-sca** implies that the supercritical-CO_2 treatment prevents dense aggregation of the polymer particles. Indeed, SEM images showed that particles of **SNU-C1-sca** were much less densely packed than those of **SNU-C1-va** (see Figure S1 in the Supporting Information). The different micropores and mesopores of **SNU-C1-va** and **SNU-C1-sca** suggest that the polymer framework responds differently, depending on the activation method used.

The CO_2-adsorption isotherms of **SNU-C1-va** and **SNU-C1-sca** were measured at 273, 285, and 298 K, and the data are summarized in Table 1. The isotherms show slight hysteresis on desorption (see Figure S10 in the Supporting Information). **SNU-C1-va** shows a CO_2 uptake of 2.31 mmol g^{-1}

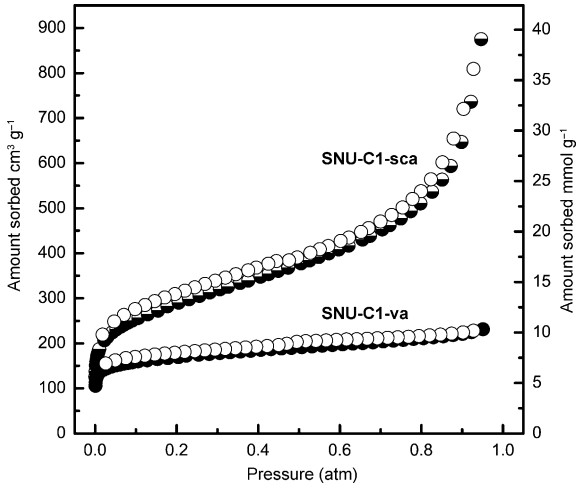

Figure 1. N_2-adsorption isotherms at 77 K for **SNU-C1-va** and **SNU-C1-sca**. Filled circles: adsorption in **SNU-C1-va**; half-filled circles: adsorption in **SNU-C1-sca**; open circles: desorption.

Table 1. Gas adsorption data of **SNU-C1-va**, **SNU-C1-sca**, and some reported clicked POPs.

Clicked-POP	Gas	T [K]	Uptake[a] [mmol g^{-1}]	BET [$m^2 g^{-1}$]	Q_{st}[b] [kJ mol^{-1}]
SNU-C1-va	N_2	77	10.36	595	–
		298	0.14	–	–
	CO_2	273	3.49	–	34.9
		285	2.77	–	–
		298	2.31	–	–
	CH_4	298	0.50	–	–
SNU-C1-sca	N_2	77	39.07	830	–
		298	0.32	–	–
	CO_2	273	4.38	–	31.2
		285	3.72	–	–
		298	3.14	–	–
	CH_4	298	0.67	–	–
HCP-5[c]	CO_2	298	1.25[d]	494	28.5
MOP-C[e]	CO_2	273	3.86	1470	33
		298	2.20	–	–

[a] At 1 atm. [b] Isosteric heat of the CO_2 adsorption at low coverage. [c] See ref. [40]. [d] Datum was obtained by digitalizing a high-pressure adsorption isotherm plot in the reference. [e] See ref. [8].

($51.8\ cm^3\ g^{-1}$) at 298 K and 1 atm (Figure 2a). The isosteric heat (Q_{st}) of the CO_2 adsorption at low coverage is $34.9\ kJ\ mol^{-1}$, as estimated using the Clausius–Clapeyron equation[6] in conjunction with the Toth-equation fitting parameters obtained from the adsorption data measured at 273, 285, and 298 K (Figure 2b). At 1 atm and at all the measured temperatures, **SNU-C1-sca** shows higher (1.26–1.36 times) CO_2 uptake than **SNU-C1-va** (Table 1). It adsorbs $3.14\ mmol\ g^{-1}$ ($70.3\ cm^3\ g^{-1}$) of CO_2 at 298 K and 1 atm. The low-coverage Q_{st} value of **SNU-C1-sca** is $31.2\ kJ\ mol^{-1}$, which is slightly lower than that of **SNU-C1-va**. The data suggest strong physisorption ($<40\ kJ\ mol^{-1}$)[42] rather than chemisorption of CO_2 in both **SNU-C1-va** and **SNU-C1-sca**. This is further supported by the fact that those materials could be fully reactivated under vacuum at room temperature after CO_2 adsorption and then subsequently being able to adsorb the same amount of gas (see Figure S14 in the Supporting Information). The low-coverage Q_{st} values of **SNU-C1-va** and **SNU-C1-sca** are quite high in comparison with that ($15.6\ kJ\ mol^{-1}$) of **PAF-1**,[43] which contains no additional functional group, and they are rather close to those of previously reported clicked POPs containing the triazole functional group, **HCP-5**[40] and **MOP-C**[8] (Table 1). Moreover, the CO_2 uptakes at 298 K and 1 atm of **SNU-C1-va** and **SNU-C1-sca** are significantly higher (1.85 and 2.51 times) than that of **HCP-5**, even when the higher (1.20 and 1.68 times) BET surface areas of **SNU-C1-va** and **SNU-C1-sca** are considered. Also, the CO_2 uptakes are even higher (1.05 and 1.43 times) than that of **MOP-C**, which has 2.47 and 1.77 times higher surface area than **SNU-C1-va** and **SNU-C1-sca**, respectively. Compared with those previously reported clicked POPs, the **SNU-C1** samples described herein contain carboxy groups in addition to the triazole groups on the pore surface. It is believed that enrichment of these moderately CO_2-attracting groups on the pore surface of **SNU-C1** enhances room-temperature CO_2 uptakes.

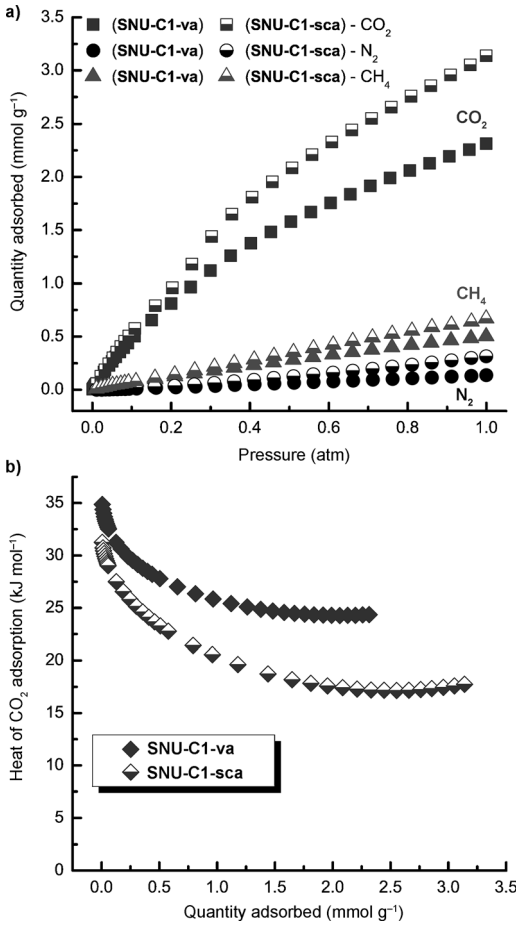

Figure 2. a) Adsorption isotherms of **SNU-C1-va** and **SNU-C1-sca** for CO_2 (squares), N_2 (circles), and CH_4 (triangles) gases at 298 K; desorption isotherms are not shown for clarity; b) isosteric heat of CO_2 adsorption in **SNU-C1-va** and **SNU-C1-sca**.

The CO_2-capture ability of SNU-C1-va and SNU-C1-sca: In general, uptake capacity and adsorption selectivity of CO_2 over other gases (for example, N_2, CH_4) have been regarded as two principle factors for evaluating CO_2-capture ability of materials. However, the regenerability of the material and the kinetics of separation cycles also need to be considered in real CO_2 capture and separation processes. Based on this consideration, Bae and Snurr have proposed five complementary parameters for better evaluating the CO_2-capture adsorbents in PSA and VSA applications.[15] These parameters are: 1) CO_2 uptake under adsorption conditions, N_1^{ads}; 2) working CO_2 capacity, $\Delta N_1 = N_1^{ads} - N_1^{des}$; 3) regenerability, $R = \Delta N_1 / N_1^{ads} \times 100$; 4) selectivity under adsorption conditions, $\alpha_{12}^{ads} = (N_1^{ads} \times y_2)/(N_2^{ads} \times y_1)$; 5) sorbent selection parameter, $S = (\alpha_{12}^{ads})^2/\alpha_{12}^{des} \times (\Delta N_1/\Delta N_2)$, where subscripts 1 and 2 stand for CO_2 and the other gas (for example, N_2 and CH_4) in the gas mixture, respectively, superscripts ads and des indicate adsorption and desorption conditions, respectively, and y_i is the molar fraction of gas i in the gas mixture to be separated. It should be noted that the comprehensive parameter S takes into account the usually ignored α_{12}^{des} and ΔN_2 values, which contribute to purity of captured CO_2.

The abilities of **SNU-C1-va** and **SNU-C1-sca** for CO_2 separation from flue gas and landfill gas by the VSA method were evaluated by using the CO_2-, N_2-, and CH_4-adsorption data measured at 298 K (Table 1 and Figure 2). The five separation parameters of the two samples were calculated using the ideal adsorbed solution theory (IAST, see the Experimental Section),[44] and they are presented in Table 2 together with the reported data of some promising adsorbents.[15] For comparison, the gas mixture having the same compositions as flue gas and landfill gas (1:9 CO_2/N_2 and 1:1 CO_2/CH_4, respectively), and VSA conditions (temperature, 298 K; adsorption and desorption pressures, 1 and 0.1 atm) were adopted in the calculations. The data reveal that there is little difference between the regenerabilities of **SNU-C1-va** and **SNU-C1-sca**. Overall, **SNU-C1-sca** shows higher working CO_2 capacities than **SNU-C1-va**. However, **SNU-C1-va** has higher selectivities and comprehensive S values than **SNU-C1-sca**. For flue-gas separation, although **SNU-C1-va** shows lower working CO_2 capacity than **Zeolite-5A**,

Table 2. VSA separation parameters of **SNU-C1-va**, **SNU-C1-sca**, and some reported adsorbents for flue gas and landfill gas.[a]

Gas mixture	Adsorbent	N_1 [mmol g^{-1}]	ΔN_1 [mmol g^{-1}]	R [%]	α_{12}^{ads}	S
Flue gas[b]	**SNU-C1-va**	0.47	0.41	87.3	38.0	262
	SNU-C1-sca	0.58	0.51	88.5	17.0	88
	ZIF-78	0.60	0.58	96.3	34.5	396
	Zeolite-5A	3.50	2.36	67.4	61.8	163
	Zeolite-13X	2.49	1.35	54.2	86.2	128
	Ni-MOF-74	4.34	3.20	73.7	41.1	83.5
Landfill gas[c]	**SNU-C1-va**	1.51	1.21	80.6	9.7	84
	SNU-C1-sca	1.99	1.60	80.4	7.5	38
	CUK-1	2.76	2.33	84.4	14.0	359
	Mg-MOF-74	7.23	2.32	32.1	12.5	23.5
	HKUST-1	2.81	1.90	67.5	5.5	19.8
	Zeolite-13X	3.97	1.97	49.6	13.2	19.1

[a] See ref. [15]. [b] 1:9 CO_2/N_2. [c] 1:1 CO_2/CH_4; for both cases, adsorption and desorption pressures are 1.0 and 0.1 atm, respectively; the VSA temperature is 298 K.

Zeolite-13X, and **Ni-MOF-74**, it has better regenerability and comprehensive S values (Table 2). It is also remarkable that the selectivity of **SNU-C1-va** is higher than **ZIF-78**, which shows the highest comprehensive S value among all the adsorbents. For landfill-gas separation, **SNU-C1-va** shows high regenerability, a large comprehensive S value, and moderate selectivity compared with **Mg-MOF-74**, **HKUST-1**, and **Zeolite-13X**, although the top-performing adsorbent, **CUK-1**, has higher values. Compared with a recently reported POP, **BILP-10**, which has CO_2 selectivities of approximately 57 and 9 for flue gas and landfill gas separation, respectively, under similar conditions,[45] the selectivity values of **SNU-C1-va** are a little bit lower than **BILP-10**.

Binary gas-cycling experiments: To test the CO_2-capture performance of **SNU-C1-va** and **SNU-C1-sca** from a gas mixture, gas-cycling experiments[13,46] were performed at 30 °C on a thermogravimetric analyzer by introducing a stream of a CO_2-N_2 mixture (15:85 *v*/*v*) followed by a pure N_2 purge. Before the experiment, the samples were dried at 60 °C with a pure N_2 stream for 5 hours to remove adsorbed moisture during the sample handling. For **SNU-C1-va**, in the first cycle, the weight was increased by approximately 1.28 wt % under the gas mixture and the increase was almost fully reversed by the N_2 purge (Figure 3a). Over 12 cycles, the weight changes were essentially identical, a behavior that reflects good regenerability and cyclability of the material. The steep slopes for weight increase and decrease during the cycles suggest rapid kinetics of gas adsorption and desorption. To test water stability of **SNU-C1-va**, the same gas-cycling experiments were performed after the material was soaked in water for 48 hours and subsequently dried at 60 °C under a pure N_2 stream for 5 hours. For the water-treated and activated sample, the weight increase caused by placing the sample under the gas mixture and the profile of the adsorption–desorption cycles were the same as those of the original sample. This result indicates that **SNU-C1-va** is highly stable in the presence of water (Figure 3a). For **SNU-C1-sca**, the weight increase (1.15 %) under the stream of the gas mixture is slightly less than that of **SNU-C1-va** (Figure 3b), even though it shows higher CO_2 uptake than **SNU-C1-va** in the single-component gas adsorption at 1 atm. After being soaked in water for 48 hours followed by activation at 60 °C under a pure N_2 stream for 5 hours, **SNU-C1-sca** shows increased weight change under the gas mixture, and the value is close to that of **SNU-C1-va** (Figure 3b). It is believed that the network structure of **SNU-C1-sca** changes to that of **SNU-C1-va**

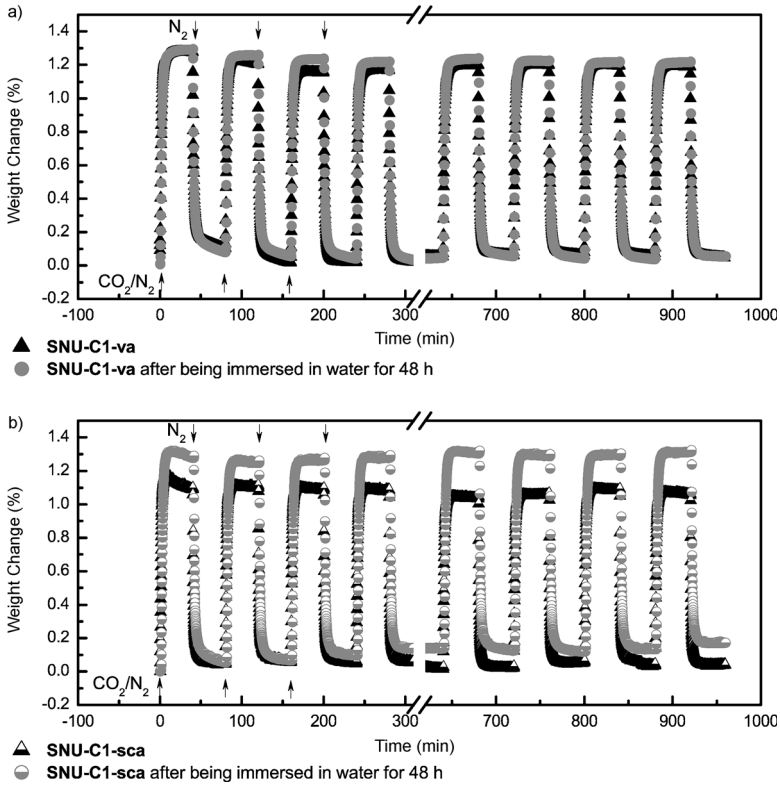

Figure 3. Gas-cycling experiments performed at 30 °C for a) **SNU-C1-va** and b) **SNU-C1-sca**. Data points for weight changes during the cycles of introduction of a CO_2/N_2 mixture (15:85 *v*/*v*) followed by a pure N_2 purge are shown as triangles. For comparison, similar experimental data for samples that were soaked in water for 48 h followed by activation with an N_2 purge at 60 °C for 5 h are shown as circles. For each cycle, the CO_2/N_2 mixture gas was introduced for 40 min and then pure N_2 gas for another 40 min. The relatively small buoyancy changes were not deduced from the data.

during the water treatment and subsequent activation. This is also supported by the color change of **SNU-C1-sca** from pale yellow to orange, which is the color of **SNU-C1-va**, after activation of the water-treated sample. We assume that drying the water-adsorbed **SNU-C1-sca** sample under 60 °C induces a structural change to the one that vacuum drying of the as-synthesized **SNU-C1** does.

Conclusion

We have synthesized a new porous organic polymer, **SNU-C1**, which contains two kinds of moderately CO_2-attracting functional moieties, carboxy and triazole groups. After **SNU-C1** was activated by the conventional evacuation method and the supercritical-CO_2 drying method, respectively, the CO_2-capture ability of each guest-free material was evaluated by the experimental sorption studies as well as calculation of five VSA separation parameters, that is, CO_2-adsorption-capacity, working-capacity, regenerability, selectivity, and sorbent-selection parameters. The results reveal that porosity and CO_2-capture performance of the POP depend upon the activation method used. In addition, the POP described herein has high CO_2-uptake capacity at room temperature, high selectivity, high regenerability, and good stability against water, and thus it has great potential application in CO_2 capture.

Experimental Section

Synthesis of SNU-C1: To a round-bottom flask (100 mL) containing 3,5-diazidobenzoic acid (**Hdab**; 0.082 g, 0.4 mmol, 1.0 equiv), 1,3,5,7-tetrakis(4-ethynylphenyl)adamantane (**tepa**; 0.107 g, 0.2 mmol, 0.5 equiv), and a magnetic stirring bar, DMSO (20 mL) was added. The flask containing the resultant clear solution was placed in a preheated 90 °C oil bath and the solution was stirred. Then, an aqueous solution (0.5 mL) of $CuSO_4{\cdot}5H_2O$ (0.020 g, 0.08 mmol, 0.2 equiv) and L-ascorbic acid (0.028 g, 0.16 mmol, 0.4 equiv) was added dropwise to the solution, which immediately became cloudy. After addition, the flask was capped with a rubber septum and the heterogeneous mixture was stirred at 90 °C for 96 h. The reaction mixture was cooled to room temperature and filtered under reduced pressure. The solid product was washed with DMSO (100 mL) and MeOH (300 mL). This as-synthesized sample of **SNU-C1** was immersed in MeOH for further activations, which are described below. Yield: 0.175 g (93 % of weight sum of the two reactants). Elemental analysis calcd (%) for $C_{56}H_{40}N_{12}O_4{\cdot}3H_2O$ ([**tepa**][**Hdab**]$_2{\cdot}3H_2O$): C 67.32, H 4.64, N 16.82; found: C 65.70, H 4.67, N 17.04 (for **SNU-C1-va**); C 65.83, H 4.55, N 16.94 (for **SNU-C1-sca**). The elemental-analysis data indicate that activated **SNU-C1** samples adsorb water from air to various degrees during the sample handling.

Activation of SNU-C1: The guest solvent molecules included in **SNU-C1** were removed by two different activation methods, namely, high dynamic vacuum activation at room temperature for 12 h, and supercritical-CO_2 treatment. Vacuum activation is a common method; supercritical-CO_2 treatment is described as follows. As-synthesized **SNU-C1** was immersed in 30 mL MeOH for 3 h, during which time, the solution was replaced with fresh MeOH three times. The sample was then transferred to a supercritical dryer together with a small amount of MeOH. The temperature and pressure of the chamber were raised to 40 °C and 200 bar with CO_2 by using a CO_2 syringe pump, above the critical point (31 °C, 73 atm) of CO_2. The supercritical CO_2 in the chamber was vented at a rate of 10 mL min^{-1} until pressurized CO_2 in the syringe pump was empty, which was then filled with CO_2 again. The cycle of refilling with CO_2, pressurizing, and venting was repeated over 8 h. Finally, the supercritical-CO_2-activated sample of **SNU-C1** was obtained as a pale yellow powder.

Gas-sorption experiments: The gas adsorption–desorption experiments were performed using an automated micropore gas analyzer, Autosorb-1 (Quantachrome Instruments). All the gases used were of 99.9999 % purity. The N_2-sorption isotherms were measured at 77 K and 298 K, CH_4-sorption isotherms were measured at 298 K, and CO_2-sorption isotherms were measured at 273 K, 285 K, and 298 K. The adsorption temperatures were achieved by using baths of liquid nitrogen (77 K), ice/water (273 K), dry ice/dioxane (285 K), and water (298 K). N_2-adsorption isotherms measured at 77 K were used for porosity analyses. Brunauer—Emmett–Teller (BET) and Langmuir surface areas were calculated from the adsorption data in the pressure range of 0.005–0.01 atm (see Figure S5 in the Supporting Information). Micropore analyses were performed by using the Dubinin–Radushkevich (DR) method[47] in the pressure range of 0.005–0.01 atm (see Figure S6 in the Supporting Information). By using nonlocal density-functional theory[41] (NLDFT), pore-size-distribution calculations were performed with the adsorption data in the pressure range of 0.005–0.025 atm and with the desorption data in the pressure range of 0.025–0.95 atm. The NLDFT equilibrium model—N_2 at 77 K on carbon (slit pore)—was used for the calculations because it provided the best fit (see Figure S7 in the Supporting Information).

Gas-cycling experiments: A sample (around 20 mg) introduced to a TA-Q50 thermogravimetric analyzer was heated at 60 °C for 5 h to remove adsorbed water under a pure N_2 flow (99.9999 %). After the temperature of the furnace was reduced and stabilized at 30 °C, a CO_2/N_2 mixture (15:85 *v*/*v*) was introduced into the furnace for 40 min and then pure N_2 was introduced for another 40 min. This cycle was repeated 12 times. A flow rate of 60 mL min^{-1} was employed for both gases. The weights of the sample were recorded during the cycles.

Estimation of isosteric heat of CO_2 adsorption: Isosteric heat of CO_2 adsorption was estimated from the CO_2-sorption data measured at 273, 285 and 298 K. Firstly, the Toth equation,[48,49] Equation (1), was used for independent fittings of the isotherms (see Figure S9 in the Supporting Information), where N is the amount of adsorbed gas in cm^3 g^{-1}, N_{sat} is the saturated adsorption amount, P is the pressure in atm, b and t are the equation constants. It is noteworthy that the Toth equation reduces to the Langmuir equation when t has the value of 1.

$$N = \frac{N_{sat} b P}{(1 + bP^t)^{\frac{1}{t}}} \tag{1}$$

Then, the expression for the pressure, P, in terms of the CO_2-adsorption amount, N, could be obtained by using Equation (2).

$$P = \frac{N}{(b^t N_{sat}^t - bN^t)^{\frac{1}{t}}} \tag{2}$$

Isosteric heats of the CO_2 adsorption (Q_{st}) were calculated with the Clausius–Clapeyron equation[6,50] Equation (3), where T is the temperature, R is the universal gas constant, and C is a constant. The Q_{st} values at different CO_2 loading, N, were obtained from the slopes of the plots of $(\ln P)_N$ as a function of $(1/T)$.

$$(\ln P)_N = -\frac{Q_{st}}{R}\frac{1}{T} + C \tag{3}$$

Calculation of CO_2-separation parameters: Ideal adsorbed solution theory (IAST)[44] enables prediction of adsorption equilibriums of the binary gas mixtures from the related single-component isotherms. According to IAST:

$$y_1 + y_2 = 1 \tag{4}$$

$$x_1 + x_2 = 1 \tag{5}$$

$$p_{mix}y_1 = p_1^o x_1 \quad (6)$$

$$p_{mix}y_2 = p_2^o x_2 \quad (7)$$

$$\pi_1^o = \frac{RT}{A}\int_0^{p_1^o} n_1(p)d\ln p \quad (8)$$

$$\pi_2^o = \frac{RT}{A}\int_0^{p_2^o} n_2(p)d\ln p \quad (9)$$

$$\pi = \pi_1^o = \pi_2^o \quad (10)$$

where y_i is the mole fraction of component i in the bulk gas mixture, x_i is the mole fraction of component i in adsorbed gas mixture, p_{mix} is the total pressure of the bulk gas mixture, p_i^o is the bulk pressure of pure component i that corresponds to the spreading pressure π of the binary mixture, R is the universal gas constant, T is adsorption temperature, A is surface area of the adsorbent, $n_i(p)$ is amount adsorbed at pressure p for pure component i.

Using Equations 4–10, the following equation can be obtained:

$$\int_0^{\frac{p_{mix}y_1}{x_1}} n_1(p)d\ln p = \int_0^{\frac{p_{mix}y_2}{1-x_1}} n_2(p)d\ln p \quad (11)$$

Total adsorbed amount of the gas mixture (n_Δ) is calculated by the following equation:

$$\frac{1}{n_\Delta} = \frac{1}{n_1(p_1^o)} + \frac{1}{n_2(p_2^o)} \quad (12)$$

where $n_1(p_1^o)$ is the amount of component 1 adsorbed at spreading pressure π in the absence of component 2, and $n_2(p_2^o)$ is the amount of component 2 adsorbed at spreading pressure π in the absence of component 1.

The adsorption amount for the component i (n_i^Δ) in the binary mixture adsorption is calculated using the following equation:

$$n_1^\Delta = n_\Delta x_1 \quad (13)$$

$$n_2^\Delta = n_\Delta x_2 \quad (14)$$

Adsorption selectivity of component 1 over component 2 (S_{12}) is calculated using the following equation:

$$S_{12} = \frac{x_1 y_2}{x_2 y_1} \quad (15)$$

For calculating the above-mentioned five CO_2 separation parameters for flue-gas separation by the VSA method, the gas-mixture composition is assumed to be 1:9 CO_2/N_2 and the adsorption and desorption pressures are assumed to be 1 and 0.1 atm, respectively; CO_2 is component 1 and N_2 is component 2. For adsorption, p_{mix} is 1 atm, y_1 is 0.1, y_2 is 0.9, and the functions $n_i(p)$ can be obtained by fittings of the single-component adsorption isotherms with single-site Langmuir–Freundlich equation (see the Supporting Information, Figure S10–13). Value x_1 can be then obtained by solving Equation (11) by using MATLAB software.[51] All other unknowns can be obtained from the value of x_1. Value n_1^Δ, obtained from Equation (13), corresponds to the CO_2 uptake under adsorption conditions, value n_2^Δ, obtained from Equation (14), corresponds to the N_2 uptake under adsorption conditions, and value S_{12}, obtained from Equation (15), corresponds to the selectivity under adsorption conditions. For desorption, p_{mix} is 0.1 atm, y_1 is 0.1, y_2 is 0.9, and the functions $n_i(p)$ can be obtained by fittings of the single-component desorption isotherms with the single-site or dual-site Langmuir–Freundlich equation (see the Supporting Information, Figure S10–13). After solving the Equation (11), all other unknowns can be obtained. Value n_1^Δ, obtained from Equation (13), corresponds to CO_2 uptake under desorption conditions, value n_2^Δ, obtained from Equation (14), corresponds to N_2 uptake under desorption conditions, and value S_{12}, obtained from Equation (15), corresponds to selectivity under desorption conditions. The difference of the n_1^Δ values, obtained under adsorption and desorption conditions, corresponds to the working CO_2 capacity. The regenerability can be obtained by the following expression: $(n_1^{\Delta^{ads}} - n_1^{\Delta^{des}})/n_1^{\Delta^{ads}} \times 100$, where the superscripts ads and des mean calculation under adsorption and under desorption conditions, respectively. The difference of the n_2^Δ values obtained under adsorption and desorption conditions corresponds to the working N_2 capacity. The sorbent selection parameter can be obtained from the following expression: $(S_{12}^{ads})^2/S_{12}^{des}(n_1^{\Delta^{ads}} - n_1^{\Delta^{des}})/(n_2^{\Delta^{ads}} - n_2^{\Delta^{des}})$, where the superscripts ads and des mean calculation under adsorption and desorption conditions, respectively. Thus, all five parameters are obtained. The five CO_2 separation parameters for landfill-gas separation by the VSA method can be obtained in the same way by using the gas-mixture composition, 1:1 CO_2/CH_4.

Acknowledgements

This work was supported by a National Research Foundation of Korea (NRF) grant funded by the Korean Government (MEST) (No. 2012–055324 and No. 2013–0000651). L. H. Xie thanks the Brain Korea 21 for offering the fellowship.

[1] H. Q. Yang, Z. H. Xu, M. H. Fan, R. Gupta, R. B. Slimane, A. E. Bland, I. Wright, *J. Environ. Sci.* **2008**, *20*, 14–27.
[2] S. Chu, *Science* **2009**, *325*, 1599.
[3] R. Notz, I. Tonnies, N. McCann, G. Scheffknecht, H. Hasse, *Chem. Eng. Technol.* **2011**, *34*, 163–172.
[4] M. Radosz, X. Hu, K. Krutkramelis, Y. Shen, *Ind. Eng. Chem. Res.* **2008**, *47*, 3783–3794.
[5] D. Bonenfant, M. Kharoune, P. Niquette, M. Mimeault, R. Hausler, *Sci. Technol. Adv. Mater.* **2008**, *9*, 013007.
[6] K. Sumida, D. Rogow, J. Mason, T. McDonald, E. Bloch, Z. Herm, T.-H. Bae, J. Long, *Chem. Rev.* **2012**, *112*, 724–805.
[7] J.-R. Li, Y. Ma, M. C. McCarthy, J. Sculley, J. Yu, H.-K. Jeong, P. B. Balbuena, H.-C. Zhou, *Coord. Chem. Rev.* **2011**, *255*, 1791–1823.
[8] R. Dawson, E. Stockel, J. R. Holst, D. J. Adams, A. I. Cooper, *Energy Environ. Sci.* **2011**, *4*, 4239–4245.
[9] H. Kim, Y. Kim, M. Yoon, S. Lim, S. M. Park, G. Seo, K. Kim, *J. Am. Chem. Soc.* **2010**, *132*, 12200–12202.
[10] H. A. Patel, S. Hyun Je, J. Park, D. P. Chen, Y. Jung, C. T. Yavuz, A. Coskun, *Nat. Commun.* **2013**, *4*, 1357.
[11] H. A. Patel, F. Karadas, A. Canlier, J. Park, E. Deniz, Y. Jung, M. Atilhan, C. T. Yavuz, *J. Mater. Chem.* **2012**, *22*, 8431–8437.
[12] A. Samanta, A. Zhao, G. K. H. Shimizu, P. Sarkar, R. Gupta, *Ind. Eng. Chem. Res.* **2012**, *51*, 1438–1463.
[13] T. M. McDonald, W. R. Lee, J. A. Mason, B. M. Wiers, C. S. Hong, J. R. Long, *J. Am. Chem. Soc.* **2012**, *134*, 7056–7065.
[14] W. Lu, J. P. Sculley, D. Yuan, R. Krishna, Z. Wei, H.-C. Zhou, *Angew. Chem.* **2012**, *124*, 7598–7602; *Angew. Chem. Int. Ed.* **2012**, *51*, 7480–7484.
[15] Y. S. Bae, R. Q. Snurr, *Angew. Chem.* **2011**, *123*, 11790–11801; *Angew. Chem. Int. Ed.* **2011**, *50*, 11586–11596.
[16] R. Banerjee, H. Furukawa, D. Britt, C. Knobler, M. O'Keeffe, O. M. Yaghi, *J. Am. Chem. Soc.* **2009**, *131*, 3875–3877.
[17] A. P. Katsoulidis, M. G. Kanatzidis, *Chem. Mater.* **2011**, *23*, 1818–1824.
[18] S. Chen, J. Zhang, T. Wu, P. Feng, X. Bu, *J. Am. Chem. Soc.* **2009**, *131*, 16027–16029.
[19] R. Dawson, D. J. Adams, A. I. Cooper, *Chem. Sci.* **2011**, *2*, 1173–1177.
[20] W. G. Lu, D. Q. Yuan, J. L. Sculley, D. Zhao, R. Krishna, H. C. Zhou, *J. Am. Chem. Soc.* **2011**, *133*, 18126–18129.
[21] R. Vaidhyanathan, S. S. Iremonger, G. K. H. Shimizu, P. G. Boyd, S. Alavi, T. K. Woo, *Science* **2010**, *330*, 650–653.
[22] M. G. Rabbani, H. M. El-Kaderi, *Chem. Mater.* **2012**, *24*, 1511–1517.
[23] N. Y. Du, H. B. Park, G. P. Robertson, M. M. Dal-Cin, T. Visser, L. Scoles, M. D. Guiver, *Nat. Mater.* **2011**, *10*, 372–375.

[24] J.-B. Lin, J.-P. Zhang, X.-M. Chen, *J. Am. Chem. Soc.* **2010**, *132*, 6654–6656.
[25] P. Chowdhury, C. Bikkina, S. Gumma, *J. Phys. Chem. C* **2009**, *113*, 6616–6621.
[26] R. Dawson, A. I. Cooper, D. J. Adams, *Prog. Polym. Sci.* **2012**, *37*, 530–563.
[27] F. Vilela, K. Zhang, M. Antonietti, *Energy Environ. Sci.* **2012**, *5*, 7819–7832.
[28] P. Kaur, J. T. Hupp, S. T. Nguyen, *ACS Catal.* **2011**, *1*, 819–835.
[29] N. B. McKeown, P. M. Budd, *Macromolecules* **2010**, *43*, 5163–5176.
[30] M. G. Schwab, B. Fassbender, H. W. Spiess, A. Thomas, X. Feng, K. Müllen, *J. Am. Chem. Soc.* **2009**, *131*, 7216–7217.
[31] M. Rose, W. Bohlmann, M. Sabo, S. Kaskel, *Chem. Commun.* **2008**, 2462–2464.
[32] H. M. El-Kaderi, J. R. Hunt, J. L. Mendoza-Cortes, A. P. Cote, R. E. Taylor, M. O'Keeffe, O. M. Yaghi, *Science* **2007**, *316*, 268–272.
[33] T. Ben, H. Ren, S. Ma, D. Cao, J. Lan, X. Jing, W. Wang, J. Xu, F. Deng, J. M. Simmons, S. Qiu, G. Zhu, *Angew. Chem.* **2009**, *121*, 9621–9624; *Angew. Chem. Int. Ed.* **2009**, *48*, 9457–9460.
[34] C. W. Tornøe, C. Christensen, M. Meldal, *J. Org. Chem.* **2002**, *67*, 3057–3064.
[35] V. V. Rostovtsev, L. G. Green, V. V. Fokin, K. B. Sharpless, *Angew. Chem.* **2002**, *114*, 2708–2711; *Angew. Chem. Int. Ed.* **2002**, *41*, 2596–2599.
[36] A. P. Nelson, O. K. Farha, K. L. Mulfort, J. T. Hupp, *J. Am. Chem. Soc.* **2009**, *131*, 458–460.
[37] L. H. Xie, M. P. Suh, *Chem. Eur. J.* **2011**, *17*, 13653–13656.
[38] J. R. Holst, E. Stockel, D. J. Adams, A. I. Cooper, *Macromolecules* **2010**, *43*, 8531–8538.
[39] P. Pandey, O. K. Farha, A. M. Spokoyny, C. A. Mirkin, M. G. Kanatzidis, J. T. Hupp, S. T. Nguyen, *J. Mater. Chem.* **2011**, *21*, 1700–1703.
[40] O. Plietzsch, C. I. Schilling, T. Grab, S. L. Grage, A. S. Ulrich, A. Comotti, P. Sozzani, T. Muller, S. Brase, *New J. Chem.* **2011**, *35*, 1577–1581.
[41] P. I. Ravikovitch, G. L. Haller, A. V. Neimark, *Adv. Colloid Interface Sci.* **1998**, *76*, 203–226.
[42] R. Vaidhyanathan, S. S. Iremonger, G. K. H. Shimizu, P. G. Boyd, S. Alavi, T. K. Woo, *Angew. Chem. Int. Ed.* **2012**, *51*, 1826–1829.
[43] T. Ben, C. Y. Pei, D. L. Zhang, J. Xu, F. Deng, X. F. Jing, S. L. Qiu, *Energy Environ. Sci.* **2011**, *4*, 3991–3999.
[44] A. L. Myers, J. M. Prausnitz, *AIChE J.* **1965**, *11*, 121–127.
[45] M. G. Rabbani, A. K. Sekizkardes, O. M. El-Kadri, B. R. Kaafarani, H. M. El-Kaderi, *J. Mater. Chem.* **2012**, *22*, 25409–25417.
[46] H.-S. Choi, M. P. Suh, *Angew. Chem.* **2009**, *121*, 6997–7001; *Angew. Chem. Int. Ed.* **2009**, *48*, 6865–6869.
[47] M. M. Dubinin, L. V. Radushkevich, *Proc. Acad. Sci. USSR* **1947**, *55*, 331.
[48] J. Tóth, *Adv. Colloid Interface Sci.* **1995**, *55*, 1–239.
[49] A. P. Terzyk, J. Chatlas, P. A. Gauden, G. Rychlicki, P. Kowalczyk, *J. Colloid Interface Sci.* **2003**, *266*, 473–476.
[50] H. H. Pan, J. A. Ritter, P. B. Balbuena, *Langmuir* **1998**, *14*, 6323–6327.
[51] *MATLAB 7.0.1*, The MathWorks Inc., Natick, Massachusetts, **2004**.

Received: May 13, 2013
Published online: July 23, 2013

